Pharm Res (2010) 27:1348–1360
DOI 10.1007/s11095-010-0125-7

RESEARCH PAPER

Phase Separation of an IgG1 Antibody Solution under a Low Ionic Strength Condition

Hirotaka Nishi • Makoto Miyajima • Hiroaki Nakagami • Masanori Noda • Susumu Uchiyama • Kiichi Fukui

Received: 5 November 2009 / Accepted: 12 March 2010 / Published online: 17 April 2010

ABSTRACT

Purpose Phase separation of monoclonal antibody A (MAb A) solution and its relation to protein self-association are studied.

Methods A phase diagram of MAb A and its dependence on ionic strength and pH were investigated. The protein self-associations were characterized by dynamic light scattering (DLS), analytical ultracentrifugation analysis (AUC) and viscosity measurement.

Results MAb A solution with a clear appearance in an isotonic ionic strength condition turned opalescent in a low ionic strength condition, followed by liquid-liquid phase separation (LLPS) into light and heavy phases. The protein concentrations of the two phases were dependent on the ionic strength and pH. The two phases became reversibly miscible when the ionic strength or temperature was increased. DLS and AUC showed that MAb A under a low ionic strength condition self-associates at a protein concentration above the critical concentration of 16.5 mg/mL. The viscosity of the heavy phase was high and dependent on the shear rate. These results indicate that attractive protein-protein interaction in the heavy phase induces LLPS.

Conclusions LLPS was induced in MAb A solution in a low ionic strength condition due to reversible protein self-association mediated mainly by attractive electrostatic interaction among the MAb A molecules in the heavy phase.

KEY WORDS low ionic strength condition · monoclonal antibody · opalescence · phase separation · self-association

Electronic Supplementary Material The online version of this article (doi:10.1007/s11095-010-0125-7) contains supplementary material, which is available to authorized users.

H. Nishi • M. Miyajima • H. Nakagami
Formulation Technology Research Laboratories, Daiichi Sankyo Co., Ltd.
1-12-1 Shinomiya
Hiratsuka, Kanagawa 254-0014, Japan

H. Nishi • M. Noda • S. Uchiyama • K. Fukui (✉)
Department of Biotechnology, Graduate School of Engineering
Osaka University
2-1 Yamadaoka
Suita, Osaka 565-0871, Japan
e-mail: kfukui@bio.eng.osaka-u.ac.jp

INTRODUCTION

Humanized monoclonal antibodies (hMAbs) have become major pharmaceutical products in the treatment of a number of major diseases such as cancer, infectious diseases, allergies, autoimmune diseases, cardiovascular diseases and inflammation. However, mainly due to the poor bioavailability of MAbs via the oral route, the majority of approved MAbs are limited to parenteral routes of administration, and patients are forced to bear frequent and chronic administration at a clinic. The development of an alternative delivery route is required to improve patient convenience and compliance. Subcutaneous (SC) administration is the preferred route because SC administration finishes in a shorter time than IV infusion, and self-administration by patients at home is also possible. For SC administration, a high MAb concentration solution is necessary because a large dose (100~200 mg) is required for treatment, and the injection volume is limited (<1.5 mL) (1).

The development of a high MAb concentration formulation is very challenging because the behavior of highly concentrated MAb solution is quite different from that of an ideal dilute solution. Generally, proteins in highly concentrated solutions tend to self-associate due to molecular crowding and the high probability of intermolecular collisions (1-4). The non-ideality observed in the highly concentrated protein solutions is related to protein self-association, which can affect properties such as protein aggregation (4), viscosity (5, 6) and appearance. The

significant contributors in protein self-association are hydrogen bonding, excluded volume effects (2), electrostatic interaction (5), van der Waals interaction (7) and hydrophobic interaction (8).

From a pharmaceutical perspective, the prevention of MAb aggregation is most important because some MAbs form reversible or irreversible aggregates (9, 10), which could impact the therapeutic effect, pharmacokinetics or immunogenicity of the protein drug (11, 12). Protein aggregates can have a non-native conformation, and this structural change may affect the immunogenicity of the protein. Reversible aggregates (9) observed in some MAbs are likely related to some diseases, such as cryoglobulinemia, macroglobulinemia, systemic autoimmune disease and hepatitis C virus infection. In these diseases, reversible aggregation and/or self-association of monoclonal serum immunoglobulins known as cryoglobulins have been observed and are believed to be associated with pathogenesis. Cryoglobulins are immunoglobulins, most frequently IgG or IgM, which show unusual behavior upon cooling. Cryoglobulins precipitate and form a condensed phase below 37°C reversibly (13). Self-association among the Fab portions of IgG might be responsible for the precipitation of cryoglobulins (14).

The high viscosity of MAb solution impairs its suitability for administration by injection (1, 5). If the viscosity of the high concentration solution is sufficiently high, the solution can not be withdrawn and expelled using the 26 or 27 gauge needles used for SC administration. Recent studies using static and dynamic light scattering (7, 15-17), analytical ultracentrifugation (3, 5), rheometry (5, 6, 18-21), membrane osmometry (17) and zeta potential measurement (7, 16, 17) have revealed the origin of the high viscosity of MAb solution at a high concentration, especially their relationship to noncovalent reversible self-association. Although the exact mechanism is still unknown, reversible self-association driven by electrostatic interaction (5), charge-dipole and dipole-dipole interactions (7, 17) among the Fab portions of IgG (22) is reported to be a major cause of the high viscosity of MAb solution at high concentrations (>100 mg/mL). Non-covalent reversible self-association of MAb may also cause an opalescent appearance of highly concentrated MAb solutions (16, 23). Interestingly, hypothetical liquid-liquid phase separation was presented based on the protein concentration dependence of the turbidity. However, liquid-liquid phase separation has not been observed (16).

The addition of precipitating agents, such as non-ionic polymers into a binary protein-water mixture, can induce phase separation (24). Widely known as Asakura and Oosawa's depletion model (25), the addition of non-ionic polymer causes an overlap of excluded shells and drives the unbalanced osmotic force, which makes attractive protein-protein interaction. Protein salting-out in a condition of high salt concentration is also known to induce phase separation. The addition of high concentrations of salt reduces the repulsive electrostatic interactions and induces protein self-association, which is associated with protein precipitation and crystallization (26-28).

As described above, the characterization of protein self-association is important not only to develop new medical treatments for diseases, but also to develop a formulation suitable for biopharmaceuticals at a high concentration. In this report, we describe the unusual behavior of a binary monoclonal antibody A (MAb A)-salt water mixture which was not observed with several other antibodies, including commercially available ones. MAb A solution at a higher concentration has an opalescent appearance in a low ionic strength condition and is separated into two phases: light and heavy. The turbidity of the solution with opalescent appearance is much greater than that expected from the Rayleigh scattering of macromolecules at a higher concentration. Additionally, it disappears reversibly by increasing the ionic strength or increasing the temperature to the point where no phase separation occurs. We also describe the relationship between the phase separation and protein self-association.

MATERIALS AND METHODS

Materials

The humanized monoclonal antibody A (IgG1 subclass, MAb A) used in this investigation to target Fas ligand was produced in a mouse myeloma (NS0) cell line and was highly purified at Daiichi Sankyo Co., Ltd., Tokyo, Japan (29). The theoretical isoelectric point (pI) of the antibody is 6.5. The protein concentration of the MAb A stock solution was 3.51 mg/mL in 10 mM sodium phosphate buffer, 140 mM sodium chloride, 0.01% polysorbate 80, pH7.4.

Sucrose, sodium chloride and polysorbate 80 were purchased from Merck KGaA (Darmstadt, Germany), Wako Pure Chemical Industries Ltd. (Osaka, Japan) and CRODA International Plc. (East Yorkshire, UK), respectively, as the excipient materials for formulation.

Sample Preparation

MAb A stock solution was concentrated up to 165 mg/mL using tangential flow filtration (TFF) equipment (Pellicon XL ultrafiltration device MWCO 30 kDa, Millipore Corporation, Billerica, MA, USA), and then the solution was extensively dialyzed against the buffer with the desired ionic strength and pH. All the buffers were composed of 5 mM sodium phosphate, 5% (w/v) sucrose, and different concentrations of sodium chloride. Polysorbate 80 concentration in MAb A stock solution was quantified using Dragendorff's reagent by the calibration curve produced

using the standard solution containing 0, 0.002, 0.005, 0.008 and 0.01% (w/v) of polysorbate 80.

Protein Concentration Measurement

The protein concentration was mainly determined by the UV absorbance at 280 nm using a UV-1600PC (Shimadzu Corporation, Osaka, Japan). In the case that an amount of sample was insufficient for the UV absorbance measurement, the protein concentration was determined by a Bicinchoninic acid (BCA) protein assay using bovine serum albumin (BSA) as a standard (Thermo Fisher Scientific Inc., Rockford, IL, USA). When MAb A was used as a standard, the slope of the calibration curve was larger than that produced by using BSA as a standard. The ratio of the slopes was 1.396. The value of the concentration determined by the BCA protein assay was divided by the number 1.396 to convert it into the MAb A concentration.

Phase Behavior Experiments

The phase diagram of MAb A was determined as a function of the protein concentration (30). The samples prepared as described in the "Sample Preparation" section were incubated at 5°C, 15°C, 25°C, 30°C, 40°C and 50°C for 3 days for a liquid-liquid phase separation (LLPS). Sodium chloride concentration was varied from 5 to 40 mM to examine the effect of the sodium chloride concentration. The pH was varied from 5.0 to 7.0 to examine the effect of the pH. After the phase separation, the protein concentrations in the light and heavy phases were determined by BCA protein assay and were changed to UV-based protein concentrations as described in the "Protein Concentration Measurement" section. All the aliquots of each phase were diluted with saline to make homogeneous and clear solutions for a reliable determination of the protein concentrations. The MAb A solution diluted with saline has a clear appearance and has absorption below 0.005 at 320 nm. The protein concentration was plotted against the temperature.

Reversibility of LLPS and the Influence of LLPS on the Antibody Properties

Reversibility of LLPS was assessed by changing the ionic strength and pH of the solution. The change in ionic strength and pH was carried out using extensive dialysis of the antibody solution. Concentrated antibody solution (approximately 25 mg/mL) in isotonic ionic strength buffer (10 mM sodium phosphate, 140 mM sodium chloride, pH 7.4) was first dialyzed against low ionic strength buffer (5 mM sodium phosphate, 5% sucrose, pH 5.5) at 5°C to induce LLPS. After confirmation of LLPS in a dialysis tube by visual inspection, antibody solution under LLPS was dialyzed in the same dialysis tube against the isotonic ionic strength buffer. This was performed to observe whether the light and heavy phases disappeared and whether the solution recovered in a homogeneous and clear state.

The influence of LLPS on the properties of MAb A was carefully checked by characterizing MAb A in the isotonic ionic strength buffer before and after LLPS. The solutions were filtered through sterile 0.22 μm Millex GV Durapore membrane filters (Millipore Corporation, Billerica, MA, USA) before measurement.

Turbidity Measurement

Concentrated antibody solution (approximately 160 mg/mL) in isotonic ionic strength buffer (10 mM sodium phosphate, 140 mM sodium chloride, pH7.4) was dialyzed against low ionic strength buffer (5 mM sodium phosphate, 20 mM sodium chloride, 5% sucrose, pH5.5). After the determination of the protein concentration by UV absorbance at 280 nm, this MAb A solution was diluted with the same low ionic strength buffer (5 mM sodium phosphate, 20 mM sodium chloride, 5% sucrose, pH5.5) to prepare the sample in the concentration range from 1.5 to 165 mg/mL by serial dilution at a dilution factor of 1.01 to 5.04.

The turbidity of the MAb A solution was measured in 13 mm glass (culture) tubes (Thermo Fisher Scientific Inc., Rockford, IL, USA) using a HACH 2100AN turbidimeter (Hach Company, Loveland, CO, USA) at 25°C and 40°C. Since the turbidimeter was calibrated using 25 mm standard glass tubes, the observed turbidities using 13 mm glass tubes required conversion using a correlation factor. The correlation factor was determined experimentally. Standard formazin solutions with 20, 100, 200 and 400 FNU (Formazin Nephelometry Units) were prepared by serial dilution of formazin turbidity standard 4,000 FNU solution. The turbidity of these standard solutions was measured using both 13 mm and 25 mm glass tubes. The correlation factor was estimated as 1.97 from the slope of the value in the 25 mm tubes to the value in the 13 mm tubes.

Dynamic Light Scattering (DLS)

The hydrodynamic diameter of MAb A was measured at 25°C in triplicate using a NicompTM 380 ZLS, PSS Nicomp particle sizing system equipped with a 50 mW DPSS laser ($\lambda = 532$ nm) as the light source (Particle Sizing Systems Inc., Santa Barbara, CA, USA). Dynamic light scattering was determined at a scattering angle of 90°, and a time-dependent fluctuation in the scattering intensity was observed. The dynamic information of the molecule was derived from an autocorrelation of the intensity trace recorded during the experiment. The mean diameter was determined in

the volume-weighted Gaussian fit mode, and the size distribution by intensity was determined in the volume-weighted NICOMP fit mode. All the buffers were filtered through sterile 0.22 μm Millex GV Durapore membrane filters (Millipore Corporation) before measurement. The measurements of MAb A, which underwent LLPS, were performed within 10 min after homogenizing the coexisting phase.

Analytical Ultracentrifugation-Sedimentation Velocity (AUC-SV)

The distributions of MAb A under a low ionic strength condition (5 mM sodium phosphate and 10 mM sodium chloride, pH5.5) and isotonic ionic strength conditions (5 mM sodium phosphate and 140 mM sodium chloride, pH5.5) were analyzed using the AUC-SV method. AUC-SV experiments were performed using Proteomelab XL-I Analytical Ultracentrifuge (Beckman-Coulter, Fullerton, CA). Samples of 25 mg/mL were measured. Runs were carried out at 12,000 rpm or 40,000 rpm at a temperature of 20.0°C using 3 mm charcoal epon double sector centerpieces and four-hole An60 Ti analytical rotor equilibrated to 20.0°C. The evolution of the resulting concentration gradient was monitored with Rayleigh interference detection optics. At least 300 scans were collected between 6.00 and 7.25 cm from the center of the rotation axis. All SV raw data were analyzed by the continuous *C(s)* distribution model using the software program SEDFIT11.71 (33). The position of the meniscus and frictional ratio (f/f_0) was set to vary as fitted parameters, and time-invariant (TI) noise and radian-invariant (RI) noise were removed. Additional parameter for the analysis that included partial specific volumes (0.728 cm^3/g), buffer density ($\rho = 0.99979$ g/cm^3 for a low ionic strength condition and $\rho = 1.00516$ g/cm^3 for an isotonic ionic strength condition) and viscosity ($\eta = 1.0067$ centipoises for low ionic strength condition and $\eta = 1.0180$ centipoises for isotonic ionic condition) was calculated using the SEDNTERP program. A resolution of 200 increments between 0 and 30 S was entered, and maximum entropy regularization was used ($p = 0.68$).

Viscosity Measurement

The viscosity of the protein sample was measured using Viscometer/Rheometer-on-a-Chip (VROC) (RheoSense Inc., San Ramon, CA, USA) at ambient temperature and Physica MCR 301 cone/plate rheometer (Anton Paar GmbH, Graz, Austria) at 25°C.

VROC consists of a rectangular slit formed of glass and a pressure sensor array and provides shear rate-dependent viscosity accurately with a small amount of sample for both Newtonian and non-Newtonian fluids (31, 32). Approximately 1 mL of MAb A solution loaded into a syringe flowed through the slit at various flow rates using a syringe pump. The pressure was plotted as a function of the position, and the wall shear stress (τ) was calculated from the slope of this plot. The viscosity was calculated from the τ value.

Physica MCR 301 cone/plate rheometer was equipped with a spindle model CP50-0.5, and approximately 1 mL of samples was loaded on the measuring plate. The temperature was controlled at 25°C via a peltier element, and a solvent trap was used to prevent solvent evaporation. The viscosity was measured over a range from 0.01 to 10,000 (s^{-1}) to evaluate the shear rate.

Newtonian and non-Newtonian behavior of the fluids can be determined from the shear rate dependence of the viscosity.

Size-Exclusion Chromatography (SEC)

The distribution of intact protein, soluble aggregate and fragments of MAb A was determined using size exclusion chromatography (SEC). An LC-10Avp high performance liquid chromatography (HPLC) system (Shimadzu Corporation) was used with a Protein KW-803 column (Showa Denko K.K., Tokyo, Japan) at a flow rate of 0.5 mL/min using 30 mM sodium phosphate buffer containing 300 mM sodium chloride, pH6.7 as the mobile phase. A 200 μg sample of protein was injected onto the column and was detected at an absorbance of 280 nm.

Ion-Exchange Chromatography (IEC)

The amount of intact IgG and its acidic variants were quantitatively determined by cation-exchange chromatography (IEC) using a ProPac WCX-10 column (Dionex Corporation, Sunnyvale, CA, USA) at a flow rate of 0.5 mL/min. The separation of variously charged species was achieved through an NaCl gradient. Mobile phase A was 10 mM sodium phosphate buffer at pH 7.0, and mobile phase B was 10 mM sodium phosphate buffer containing 1.0 M sodium chloride at pH7.0. The mobile phase mixture varied from 6% initially to 9% at 34 min, up to 50% from 34 min to 45 min and finally back to 6% from 45 min to 60 min. One-hundred μg of protein was injected onto the column and detected at an absorbance of 280 nm.

Enzyme-Linked Immunosorbent Assay (ELISA)

A 96-well Nunc-Immuno plate (Nalge Nunc International K.K., Tokyo, Japan) was coated with the target protein, stored overnight at 4°C and blocked with diluted Immuno Block (Dainippon Sumitomo Pharma Co., Ltd., Osaka, Japan), followed by washing with rinse solution three times. Then MAb A and horseradish peroxidase-labeled goat anti-

human IgGκ antibody (Bethyl Laboratories, Inc., Montgomery, TX, USA) were added to the plate, followed by incubation for 1 h at ambient temperature. After washing four times, o-Phenylenediamine (OPD) (Wako Pure Chemical Industries Ltd.) solution and hydrogen peroxide (Wako Pure Chemical Industries Ltd.) were added and incubated for 30 min. The enzymatic reaction was stopped by adding diluted sulfuric acid (Wako Pure Chemical Industries Ltd.), and the UV absorbance at 492 nm was measured with a GENIOS multi-plate reader (Tecan Japan Co., Ltd., Kanagawa, Japan). The calibration curve was determined with the MAb A standard solution at the concentration of 0, 4, 8, 12, 16 and 20 ng/mL. The ratio of ELISA-based protein concentration to total protein concentration was evaluated as the binding ability of MAb A to the target chimera protein, which is composed of human Fas ligand conjugated with Fc (human Fas-Xa-Fcγ1).

RESULTS

The solution pH and ionic strength have a significant effect on the solution behavior of MAb A, as well as on its physical and chemical stabilities. To evaluate the effect, the solution condition was exchanged by dialysis from an isotonic ionic strength condition (10 mM sodium phosphate, 140 mM sodium chloride, pH7.2) to a low ionic strength condition (5 mM sodium phosphate, 10 mM sodium chloride, 5% sucrose, pH5.5). Even though MAb A solution of 2.25 mg/mL has a clear appearance at ambient temperature (≈2 FNU), it gradually becomes opalescent at 5°C (≈80 FNU) (Fig. 1). This opalescent solution at 5°C became clear reversibly at ambient temperature. A similar behavior of the highly concentrated lysozyme solution was previously reported (34, 35). This phenomenon of MAb A solution was not observed in an isotonic ionic strength condition. At a higher concentration (107.22 mg/mL), the opalescent and homogeneous MAb A solution separated into two phases in a lower ionic strength condition (5 mM sodium phosphate, 10 mM sodium chloride, 5% sucrose, pH5.5) at ambient temperature. Fig. 2 shows the time-dependent change in its appearance in a glass vial. After storage at ambient temperature for up to 2 days, the solution gradually separated into two phases, and finally the coexisting phase appeared, and liquid-liquid interface could be observed (Fig. 2d). The upper phase and the lower phase were named light and heavy phases, respectively. The protein concentration measured in each phase showed that MAb A was highly concentrated in the heavy phase, while it has a lower concentration in the light phase, as will be described later. These results indicate that a binary MAb A-salt water mixture undergoes LLPS in low ionic strength buffer, as shown in Fig. 2. Although MAb A stock solution (165 mg/mL) contained 0.08% of polysorbate 80, polysorbate 80 concentrations up to 0.1% (w/v) have no impact on the MAb A concentrations in the light and heavy phases after phase separation at 25°C (Fig. S1). Therefore, it can be concluded that the presence of polysorbate 80 below 0.1% (w/v) has no effect on the LLPS of MAb A. In the following experiments, polysorbate 80 concentrations were not controlled but were below 0.08% (w/v).

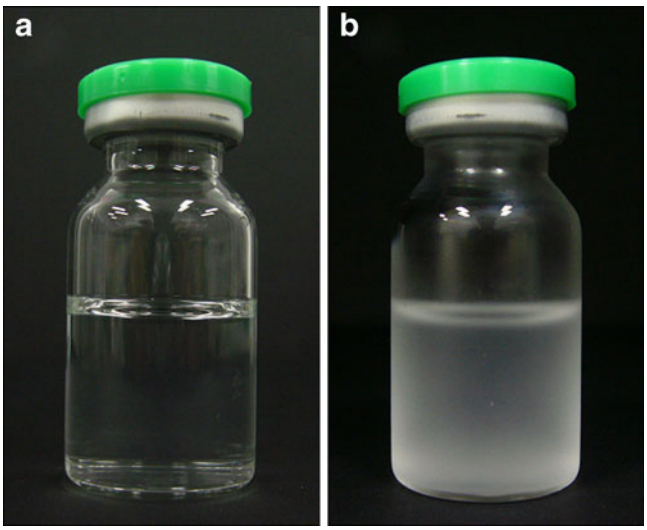

Fig. 1 Visual appearance of MAb A solution at 2.25 mg/mL in low ionic strength buffer of 5 mM sodium phosphate, 10 mM sodium chloride, 5% sucrose, pH5.5. **a**: at ambient temperature, **b**: at 5°C.

Fig. 3 shows the phase diagram of the binary MAb A-salt water mixture determined experimentally at 5 mM sodium phosphate, 5% sucrose, pH5.5 in the presence of 5, 10, 20 and 40 mM sodium chloride. The protein concentrations in the light and heavy phases were bounded by binodal curves. These binodal curves represent the protein concentrations of the coexisting phase as a function of the temperature. Fig. 3 also shows the effect of the sodium chloride concentration. The upper consolute temperature of the binary MAb A-salt water mixture depends on the sodium chloride concentration. LLPS was observed from 5°C to 50°C at a sodium chloride concentration of 5 and 10 mM. However, at a sodium chloride concentration of 20 mM, LLPS was not observed above 40°C. At a sodium chloride concentration of 40 mM, LLPS was observed at only 5°C. These results indicated that increasing the sodium chloride concentration vertically shifts the critical temperature downwards.

In order to confirm that the current LLPS is an equilibrium process, phase separation experiments were performed at different MAb A initial concentrations at 5°C and 25°C. MAb A solutions of 65, 32.5, 16.25 and 8.13 mg/mL in a buffer of 10 mM sodium phosphate,

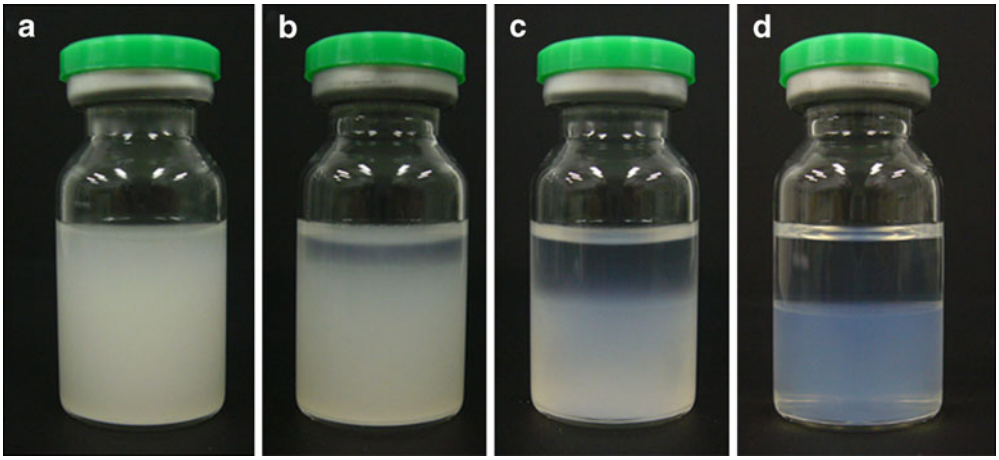

Fig. 2 Time course of visual appearance of MAb A solution at 107.22 mg/mL in low ionic strength buffer of 5 mM sodium phosphate, 10 mM sodium chloride, 5% sucrose, pH5.5 at ambient temperature after **a**: 0 min, **b**: 5 min, **c**: 20 min, **d**: 2 days.

140 mM sodium chloride, pH7.4 were dialyzed against low ionic strength buffer of 5 mM sodium phosphate, 10 mM sodium chloride, 5% sucrose, pH5.5 and induced LLPS. As shown in Fig. 4, the protein concentrations of the light and heavy phases were constant regardless of the initial protein concentration before phase separation, leading to a different volume in each phase (Fig. S2). These results indicate that LLPS is an equilibrium process, and the initial concentration has no effect on the final concentrations of each phase. The protein concentrations were 1.69 mg/mL for the light phase and 215 mg/mL for the heavy phase at 5°C, and 10.7 mg/mL for the light phase and 136 mg/mL for the heavy phase at 25°C. These concentration values are nearly the same as those determined from the binodal curve shown in Fig. 3.

The effect of pH on the phase diagram of the binary MAb A-salt water mixture was also examined. Fig. 5 shows the pH dependence of the phase diagram in 5 mM sodium phosphate, 10 mM sodium chloride, 5% sucrose. The upper consolute temperature of MAb A-salt water mixture depends on the solution pH. At pH6.5, which corresponds to the theoretical pI of the protein (pI: between 6.55 and 7.35), the area under the binodal curve was the largest.

As can be expected from the result shown in Fig. 3, MAb A is completely miscible when its concentration in the binary mixture with water solvent containing 5 mM sodium phosphate, 20 mM sodium chloride, 5% sucrose (pH5.5) is less than 22.6 mg/mL or more than 135 mg/mL at 25°C. On the other hand, over the concentration range between 22.6 and 135 mg/mL at the same temperature, the MAb A solution is expected to separate into two phases. Fig. 6 shows the turbidity of the MAb A solution as a function of the protein concentrations at 25°C and 40°C. As shown in Fig. 6, in the concentration range between 1.5 and 28 mg/mL, the turbidity of the MAb A solution in low ionic strength buffer at 25°C dramatically increased when the protein concentration increased above 20 mg/mL. On the other hand, the turbidity increased linearly with concentrations in the concentration range between 1.5 and 20 mg/mL. In the concentration range between 30 and 118 mg/mL, the turbidity at 25°C was very high and beyond the upper limit of determination. At 40°C, the

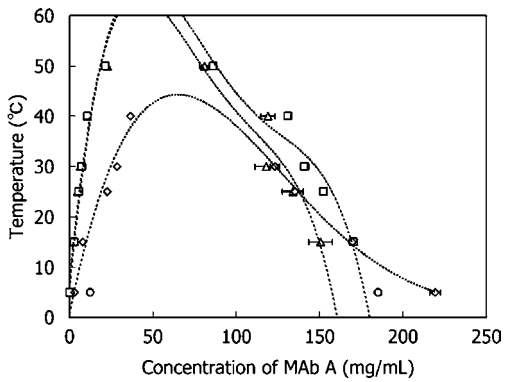

Fig. 3 Phase diagram of MAb A solution at 5 mM (△), 10 mM (□), 20 mM (◇) and 40 mM (○) of sodium chloride in 5 mM sodium phosphate, 5% sucrose, pH5.5. Note that all trend lines were fitted by polynomial curves on Microsoft Excel (33). $R^2 = 0.9721$ (△, 5 mM), $R^2 = 0.9622$ (□, 10 mM), $R^2 = 0.9748$ (◇, 20 mM). $N = 3$.

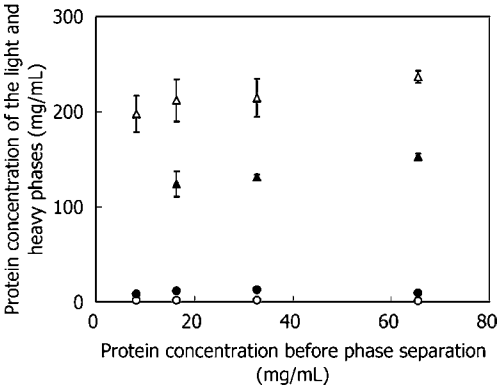

Fig. 4 Effect of the initial MAb A concentration before phase separation on the protein concentrations of the light phase at 5°C (○) and 25°C (●), and of the heavy phase at 5°C (△) and 25°C (▲) in low ionic strength buffer of 5 mM sodium phosphate, 10 mM sodium chloride, 5% sucrose, pH5.5. $N = 3$.

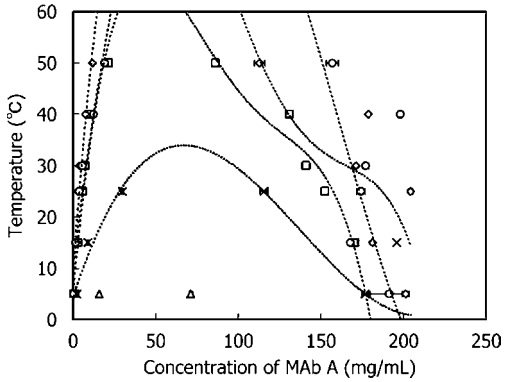

Fig. 5 Phase diagram of MAb A solution at pH5.0 (△), 5.5 (□), 6.0 (◇), 6.5 (○) and 7.0 (×) in 5 mM sodium phosphate, 10 mM sodium chloride, 5% sucrose. Note that all trend lines were fitted by polynomial curves on Microsoft Excel (33). $R^2 = 0.9622$ (□, pH5.5), $R^2 = 0.7664$ (◇, pH6.0), $R^2 = 0.8047$ (○, pH6.5), $R^2 = 0.9762$ (×, pH7.0). $N = 3$.

turbidity reached a maximum over the concentration range from 68 to 91 mg/mL. Above 91 mg/mL, the turbidity was further decreased.

The intermolecular interactions of MAb A were investigated by DLS measurement and viscosity measurement. Typical autocorrelation function was provided as shown in Fig. S3. Fig. 7 shows the mean hydrodynamic diameter of MAb A determined in volume-weighted Gaussian fit mode, (A) the size distribution of MAb A determined in volume-weighted NICOMP fit mode, (B) as a function of the protein concentration in low ionic strength buffer of 5 mM sodium phosphate, 20 mM sodium chloride, 5% sucrose, pH5.5 and in isotonic ionic strength buffer of 10 mM sodium phosphate, 140 mM sodium chloride, 5% sucrose, pH5.5 at 25°C. As shown in Fig. 7A, the mean hydrodynamic diameter of MAb A in low ionic strength buffer dramatically increased when the protein concentration increased above 16.5 mg/mL, whereas no protein concentration dependence on the mean hydrodynamic diameter was observed below 16.5 mg/mL. This critical concentration of 16.5 mg/mL corresponds to the protein concentration (≈23 mg/mL) in the light phase in the same buffer, as shown in Fig. 3. MAb A had an apparent hydrodynamic diameter of 17–21 nm below 16.5 mg/mL in low ionic strength buffer, which is slightly larger than IgG monomer. The larger value of the hydrodynamic diameter in low ionic strength buffer may result from protein self-association. This concentration dependence of the mean hydrodynamic diameter is similar to that of the turbidity for the MAb A solution in low ionic strength buffer below 28 mg/mL, as shown in Fig. 6. On the other hand, in isotonic ionic strength buffer, no protein concentration dependence on the mean hydrodynamic diameter was observed, and MAb A had a hydrodynamic diameter of 11–18 nm over the protein concentration range from 5 to 32 mg/mL.

The size distributions of MAb A were determined using volume-weighted NICOMP fit mode. As shown in Fig. 7B, MAb A showed two peaks with a hydrodynamic diameter above 16.5 mg/mL, whereas MAb A showed one peak below 11 mg/mL. As described above, the mean hydrodynamic diameter of MAb A increased with protein concentrations above 16.5 mg/mL. These results indicate that MAb A solution undergoes LLPS and small particles are formed above the critical concentration of 16.5 mg/mL.

Then, AUC-SV measurement was performed to analyze the distribution states of MAb A under low and isotonic ionic strength conditions. AUC-SV is a well-established method to analyze distribution state of proteins (36, 37) and also to quantify small soluble antibody oligomers (38, 39). The C(s) analysis of the antibody under an isotonic ionic strength condition showed that 98% of the antibody has an s-value of 7 S, which is close to the value for IgG monomer. On the other hand, larger species with 8 S, 14 S and 22 S were detected without 7 S species under a low ionic strength condition.

The viscosity of the MAb A solution was dependent on the protein concentration and the sodium chloride concentration. Fig. 8 shows the viscosity of the concentrated MAb A solution in low ionic strength buffer of 5 mM sodium phosphate, 20 mM sodium chloride, pH5.5 with or without 5% sucrose, and in isotonic ionic strength buffer of 10 mM sodium phosphate, 140 mM sodium chloride, pH5.5 at ambient temperature. Fig. 8 also shows the viscosity of the MAb A solution at a low protein concentration in low ionic strength buffer of 5 mM sodium phosphate, 20 mM sodium chloride, 5% sucrose, pH5.5. The viscosity was measured by VROC and Physica MCR 301 cone/plate rheometer. Apparently, the sodium chloride concentration had a high impact on the viscosity of the concentrated MAb A solution. According to the viscosity measured by VROC, the decrease of the sodium chloride concentration from 140

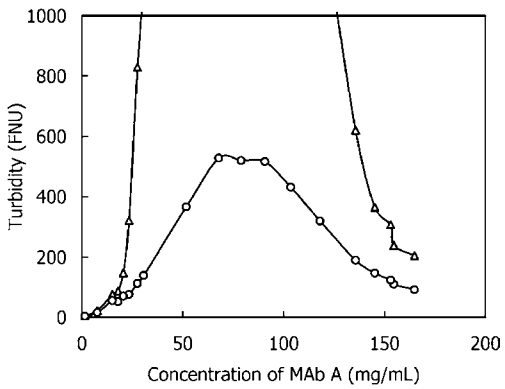

Fig. 6 Turbidity of MAb A solution over a protein concentration range between 1.5 and 165 mg/mL at 25°C (△) and 40°C (○) in low ionic strength buffer of 5 mM sodium phosphate, 20 mM sodium chloride, 5% sucrose, pH5.5. $N = 3$.

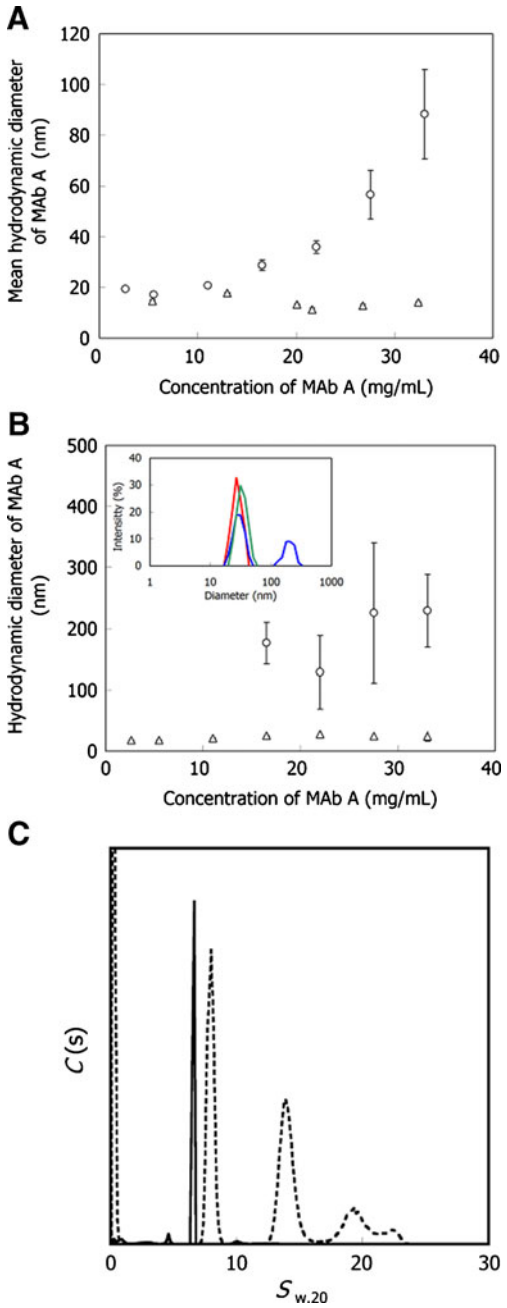

Fig. 7 (**a**) Mean hydrodynamic diameter of MAb A at 25°C that was determined in a volume-weighted Gaussian fit mode over a protein concentration range between 2.6 and 33 mg/mL in low ionic strength buffer of 5 mM sodium phosphate, 20 mM sodium chloride, 5% sucrose, pH5.5 (○); and a protein concentration range between 5.4 and 32 mg/mL in isotonic ionic strength buffer of 5 mM sodium phosphate, 140 mM sodium chloride, 5% sucrose, pH5.5 (△). (**b**) Hydrodynamic diameter of MAb A at 25°C that was determined in a volume-weighted NICOMP fit mode over a protein concentration range between 2.6 and 33 mg/mL in low ionic strength buffer of 5 mM sodium phosphate, 20 mM sodium chloride, 5% sucrose, pH5.5. The inset is the size distribution of MAb A in the same buffer at 16.5 mg/mL under LLPS (blue line) and after removal of a heavy phase (green line). The red line shows the size distribution of a MAb A monomer. The hydrodynamic diameter of MAb A observed as one or two peaks in the DLS measurement was plotted as a MAb A monomer (△) at approximately 23 nm, and self-associated MAb A (○) at approximately 190 nm. The value of the hydrodynamic diameter of MAb A monomer under LLPS was measured after removal of the heavy phase. N = 3. (**c**) C(s) Sedimentation coefficient distribution obtained from AUC-SV experiments for 25 mg/mL MAb A solution under an isotonic ion strength condition (solid line) and a low ion strength condition (dashed line).

to 20 mM raised the viscosity of the solution from 6.5 to 41 (cP) at the shear rate of 2,000 (s^{-1}). On the other hand, sucrose had little effect on the viscosity, and the viscosity of the heavy phase with or without sucrose had almost the same viscosity. Interestingly, the viscosity of the concentrated MAb A solution in low ionic strength buffer was dependent on the shear rate, and the increase of the shear rate resulted in the decrease of the viscosity, which is a typical behavior of a non-Newtonian fluid. Though the non-Newtonian behavior of a monoclonal antibody is unusual, it was reported by Liu *et al.* (5).

In order to evaluate the shear rate dependence of the viscosity over a wide range, Physica MCR 301 cone/plate rheometer was used. As shown in Fig. 8, the viscosity of the highly concentrated MAb A solution in low ionic strength buffer of 5 mM sodium phosphate, 20 mM sodium chloride, pH5.5 with or without sucrose showed apparent shear rate dependence at a shear rate below 1 (s^{-1}), and the viscosity decreased with an increase of shear rate. Sucrose had some effect on the viscosity at low shear rate. At a shear rate around 10–10,000 (s^{-1}), slight shear rate dependence was also observed. Sodium chloride concentration dependence of the viscosity was also observed when cone/plate rheometer was used. The decrease of the sodium chloride concentration from 140 to 20 mM raised the viscosity of the solution from 5.5 to 55 (cP) at the shear rate above 10 (s^{-1}). At the shear rate below 0.1 and 3.8 (s^{-1}) in measuring the viscosity of highly concentrated MAb A solution in isotonic ionic strength buffer and of low concentration MAb A solution in low ionic strength buffer, respectively, the torque was too small to measure the viscosity accurately. In the case of the MAb A solution at a low protein concentration in low ionic strength buffer, the viscosity was independent of the shear rate.

In order to evaluate the effects of LLPS on the stability of MAb A, size exclusion chromatography (SEC), ion-exchange chromatography (IEC) and ELISA measurement were performed. The results are summarized in Table I, where the aggregate contents, area % of the acidic variant peaks and binding ability are provided. SEC chromatogram is shown in Fig. S4. The binding ability was evaluated by the ratio between the ELISA-based concentration and the total protein concentration. As described in the "Materials and Methods" section, aliquots of MAb A

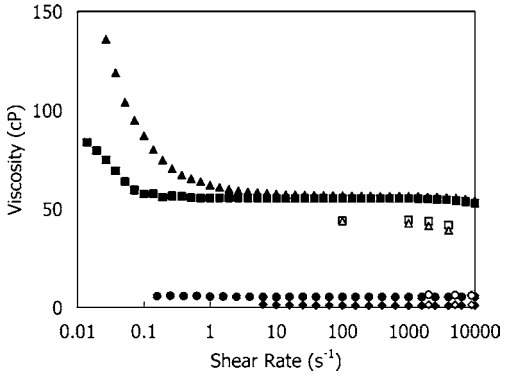

Fig. 8 Viscosity of MAb A solution and its dependence on the shear rate were measured by using VROC or Physica MCR 301 cone/plate rheometer. *Open symbols* show the viscosity obtained by VROC. *Closed symbols* show the viscosity obtained by Physica MCR 301 cone/plate rheometer: at a protein concentration of 147 (□), 155 (■), 8.8 (◇) and 8.3 (◆) mg/mL in low ionic strength buffer of 5 mM sodium phosphate, 20 mM sodium chloride, 5% sucrose, pH5.5; 156 (△) and 159 (▲) mg/mL in low ionic strength buffer of 5 mM sodium phosphate, 20 mM sodium chloride, pH5.5; and 130 (○) and 133 (●) mg/mL in isotonic ionic strength buffer of 10 mM sodium phosphate, 140 mM sodium chloride, pH5.5.

solution were taken as samples before and after LLPS. The aggregate content of the MAb A solution after LLPS did not increase, even though MAb A was concentrated once to more than 160 mg/mL during LLPS. Instead, the protein aggregate decreased slightly after phase separation. For one reason, dialysis may have some effects, such as adsorption of aggregates on the dialysis membrane. The area % of the acidic variant peak did not change during LLPS either. The binding ability was almost 100%. These results indicate that the intrinsic properties (monomer content, chemical composition and the binding ability) of MAb A are maintained after LLPS.

DISCUSSION

The scope of this study was to investigate the phase behavior of MAb A solution. The phase behavior of monoclonal antibody has been of interest mainly from the point of view of protein crystallization (26-28). In recent studies, it has been pointed out that the crystallization process of protein is affected by LLPS. During the crystallization process, nucleation occurs mostly via LLPS and crystal growth. The so-called "crystallization slot" is the restrictive slot in which the second virial coefficient is negative (40, 41).

Protein phase behavior is also related to diseases such as cryoglobulinemia and cataracts. In cryoglobulinemia, precipitates of cryoglobulin composed of IgG and/or IgM form a condensed phase upon cooling below 37°C reversibly in a low ionic strength condition, which is believed to be related to the disease (13). We found that clear and homogeneous MAb A solution in an isotonic ionic strength condition separated into two phases in a low ionic strength condition. Furthermore, the two phases became miscible by buffer exchange to isotonic ionic strength buffer or by increasing the solution temperature (Figs. 1 and 2). This phase behavior of MAb A solution is very similar to that of cryoglobulin; therefore, MAb A can be a model molecule of cryoglobulin (13, 14). In cataracts, the interaction between crystallin, an important eye lens protein, and minor constituents, such as cytoskeletal proteins and intermediate filaments, is modified with aging, and phase separation for eye crystallin is induced (42). In previous studies, a binary lysozyme-salt water mixture showed opacity upon cooling from 25°C to 12°C, and a resemblance to eye crystallin was noted (34, 35). Recently, Cromwell *et al.* reported the phase separations of an IgG monoclonal antibody (43, 44). Salinas *et al.* also suggested the phase separations of an IgG monoclonal antibody, although they did not observe obvious phase separation. The phase behavior of MAb A solution, which has a clear appearance at ambient temperature and turns opalescent at 5°C, is similar to the behavior of these proteins. Except for these proteins, no phase separation has been observed for a protein-salt water mixture. It is notable that the MAb A solution underwent LLPS without precipitating agents, such as polyethylene glycol (PEG). In addition, in this research, a solution that was not clear (>3 NTU) was described as a solution with an opalescent appearance. Meanwhile, the turbidity corresponded to the nephelometric turbidity and was used for the quantitative expression of the solution with an opalescent appearance.

The phase behavior of MAb A solution can be summarized in a phase diagram (Figs. 3 and 5). The phase diagram was investigated by changing the temperature, ionic strength and pH when LLPS was induced. MAb A exhibited a UCST (upper critical solution temperature)-type phase diagram at every sodium chloride concentration in which the protein concentration in the light phase increased and the protein concentration in the heavy phase decreased when the temperature becomes higher (Fig. 3). A similar observation was previously reported for a ternary

Table I Summary of the Quality Evaluation Before LLPS and After Redissolution of the Coexisting Phase

	Aggregate	Acidic variant peak area	Binding ability[a]
Before LLPS	2.88 ± 0.1%	18.64%	98%
After redissolution	2.58 ± 0.2%	18.91%	98%

[a] The ratio of ELISA-based protein concentration to total protein concentration was evaluated as the binding ability of MAb A to the target protein.

IgG-PEG–water mixture, where a cloud point measurement was performed (30). The upper consolute temperature of the MAb A-salt water mixture depended on the sodium chloride concentration and pH (Figs. 3 and 5). It was highest in a low ionic strength condition and near pI of the protein. These observations indicate that electrostatic interaction plays a major role in inducing LLPS.

In order to understand the phase behavior in detail, phase separation was induced in MAb A solutions at various protein concentrations. The protein concentrations of the two phases were constant even when the initial protein concentrations of the solution before LLPS were different (Fig. 4). These results suggest that this phenomenon is in fact LLPS. The concentration dependence of the turbidity of MAb A solution as a function of the protein concentrations at 25°C and 40°C are shown in Fig. 6. Although turbidity has almost the same meaning as opalescence, here, turbidity was defined as nephelometric turbidity. Nephelometric turbidity measurements detect Rayleigh scatter, which is expected to change linearly with concentration in the absence of protein self-association (23). As shown in Fig. 6, the turbidity of the MAb A solution in low ionic strength buffer dramatically increased when the protein concentration increased above the critical concentration of 20 mg/mL, whereas the turbidity increased linearly below 20 mg/mL. Although the turbidity also increases in the presence of aggregation, the turbidity of the MAb A solution in low ionic strength buffer reached a maximum and then was decreased further. These results indicate that the increase of turbidity is not due to protein (irreversible) aggregation, but due to LLPS. Inside the binodal curve, just after dispersing the heavy phase in the light phase, the heavy phase exists as small particles and scatters the light. Therefore, the high Rayleigh scatter results in the dramatic increase of the turbidity above the critical concentration of 20 mg/mL.

The mean hydrodynamic diameter of MAb A in low ionic strength buffer increased when the protein concentration increased above 16.5 mg/mL, while its protein concentration dependence was not observed below 16.5 mg/mL. This increase in the mean hydrodynamic diameter with protein concentrations above 16.5 mg/mL is similar to the concentration dependence of the turbidity, which dramatically increased when the protein concentration increased above 20 mg/mL. Sukumar *et al.* also observed a protein concentration-dependent increase in the mean hydrodynamic diameter of IgG1, where the solution had an opalescent appearance at 5°C (23). The hydrodynamic diameter of MAb A with 17–21 nm below 16.5 mg/mL corresponds to the value of IgG monomer. These results suggest that the protein self-association behavior changes around the critical concentration of 16.5 mg/mL. Considering that the protein concentration in the light phase is close to the critical concentration, the protein self-association is insignificant in the light phase, and MAb A homogeneously exists as a monomer. On the other hand, in the heavy phase, attractive intermolecular interactions play a major role in inducing LLPS. The protein-protein attractive interaction is also supported by the appearance of an additional peak at approximately 190 nm in the DLS measurement (Fig. 7B).

Consistent with the result from DLS measurement, AUC-SV analysis indicated self-association of the antibody under low ionic strength condition. The solution concentration measured (25 mg/mL) is considered to be higher for the accurate analysis under a non-ideal effect; however, it can be concluded that the majority of the antibody under low ionic strength self-associates with the s-value between 8 S–22 S, which is larger than that under the isotonic ionic strength (7 S). It should be noted that the antibody oligomers with 22 S can be estimated as a hexamer, assuming that the oligomer has the same frictional ratio as a monomer ($f/f_0 = 1.5$) and that oligomers or aggregates that have a higher s-value than 25 S are absent under a low ionic strength condition.

Thus, both the DLS and AUC results indicate the attractive intermolecular interactions among MAb A molecules under a low ionic strength condition.

Dependence of ionic strength and pH dependence on the viscosity of monoclonal antibody solutions has been investigated by other groups. It was described that the viscosity of monoclonal antibody solutions was highest at pI at a low ionic strength condition (5, 7, 17). Electrostatic interaction and charge-dipole and dipole-dipole interactions were suggested to play major roles in protein self-association. The viscosity of the MAb A solution was also highly dependent on the sodium chloride concentration, and a decrease of the sodium chloride concentration raised viscosity (Fig. 8). This result indicates that MAb A self-associates in a low ionic strength condition (7). Furthermore, the viscosity of the heavy phase in low ionic strength buffer with or without 5% sucrose was dependent on the shear rate (Fig. 8). Shear rate-dependent behavior of viscosity is a characteristic feature of non-Newtonian fluids and occurs when several micro-structural species that are made of large and elongated aggregates exist (5). Therefore, these results support the idea that self-association of MAb A mediated mainly by attractive electrostatic interaction among the MAb A molecules in the heavy phase is responsible for inducing LLPS. The viscosity of the light phase in low ionic strength buffer was independent of the shear rate (Fig. 8). Compared with the value measured by using Physica MCR 301 cone/plate rheometer, VROC showed lower viscosity than Physica MCR 301 cone/plate rheometer for non-Newtonian fluid samples. Different shear stress originating from two different measuring

methods may cause a difference in the viscosity of non-Newtonian solutions.

LLPS can be applied to the purification of monoclonal antibodies or the manufacturing of a liquid high concentration formulation. So far, these processes have usually been performed with precipitating agents such as PEG, polyvinylsulfonic acid (PVS), polyacrylic acid (PAA) and polystyrenesulfonic acid (PSS). These macromolecules are required to be subsequently removed (45, 46). However, in the case of antibodies having LLPS properties as MAb A does, the purification and concentration steps can be completed without using precipitating agents. It is possible to dilute the MAb solution with water or low ionic strength buffer and also cool the solution in a large scale. Therefore, purifying and concentrating the MAb solution can be achieved easily in the manufacturing process. For these purposes, the quality of the antibodies should be preserved during LLPS. In fact, our present study shows that LLPS of MAb A can produce a highly concentrated phase without changing its physical and chemical properties, and binding ability (Table I). No formation of an insoluble precipitation was observed during LLPS as confirmed by the turbidity measurement after adjusting the solution to an isotonic ionic condition, and by the absence of pellets after centrifugation at 20,000 g for 30 min. The recovery of MAb A after LLPS was approximately 100%. These results further demonstrate the usefulness of LLPS for antibody purification and concentration.

In Fig. 9, we proposed the pathway for LLPS induced in a binary MAb A-salt water mixture at a low ionic strength condition. Inside the binodal curve, small particles of weakly associated antibodies were formed and gradually grew to large particles. Since the density of an antibody is larger (1.3–1.4 kg/L) (23) than water, particles with a larger partial concentration of antibody form the lower part of the LLPS. Such cluster formation in a protein solution is highly interesting from the viewpoint of understanding various disease processes and producing photonic crystals (47), although the theoretical background for a high concentration solution having a non-ideal behavior is still under development.

CONCLUSIONS

Binary MAb A-salt water mixture underwent LLPS in low ionic strength buffer without a third component, i.e., precipitating agents. The two phases of the MAb A solution became reversibly miscible by increasing the ionic strength or increasing the temperature. The phase diagram and its dependence on the salt concentration and pH indicate that electrostatic interaction plays a major role in inducing LLPS. Above the critical concentration of 16.5 mg/mL, which corresponds to the protein concentration in the light phase, the mean hydrodynamic diameter of MAb A increased with the protein concentration only in a low ionic strength condition. This result is supported by the fact that MAb A self-associates to form oligomers from the AUC-SV analysis. The viscosity of the concentrated MAb A solution was highly dependent on the ionic strength. The heavy phase had high viscosity in a shear rate-dependent manner, which is characteristic of a non-Newtonian fluid. These results indicate that attractive self-association in the heavy phase is responsible for inducing LLPS. The physical, chemical and immunological properties of MAb A were unaffected by LLPS. LLPS observed in a binary MAb A-

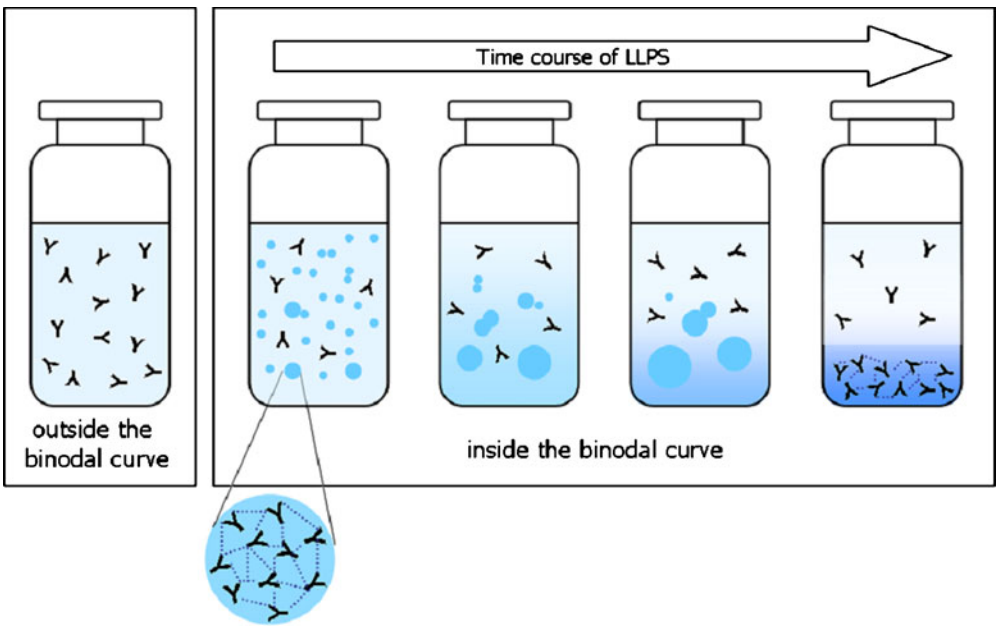

Fig. 9 Time course of LLPS induced in a binary MAb A-salt water mixture in a low ionic strength condition.

salt water mixture can be used not only to understand disease processes, but also to develop novel processes in biopharmaceuticals.

ACKNOWLEDGEMENTS

We would like to thank Mr. Yuichi Shinozaki and Ms. Tazuko Watanabe (Anton Paar Japan K.K.) for the viscosity measurements.

REFERENCES

1. Shire SJ, Shahrokh Z, Liu J. Challenges in the development of high protein concentration formulations. J Pharm Sci. 2004;93:1390–402.
2. Minton AP. Molecular crowding: analysis of effects of high concentrations of inert consolutes on biochemical equilibria and rates in terms of volume exclusion. Methods Enzymol. 1998;295:127–49.
3. Jiménez M, Rivas G, Minton AP. Quantitative characterization of weak self-association in concentrated solutions of immunoglobulin G via the measurement of sedimentation equilibrium and osmotic pressure. Biochemistry. 2007;46:8373–8.
4. Demeule B, Lawrence MJ, Drake AF, Gurny R, Arvinte T. Characterization of protein aggregation: the case of a therapeutic immnoglobulin. Biochem Biophys Acta. 2007;1774:146–53.
5. Liu J, Nguyen MDH, Andya JD, Shire SJ. Reversible self-association increases the viscosity of a concentrated monoclonal antibody in aqueous solution. J Pharm Sci. 2005;94:1928–40.
6. Saluja A, Badkar AV, Zeng DL, Nema S, Kalonia DS. Application of high-frequency rheology measurements for analyzing protein-protein interactions in high concentration solutions using a model antibody (IgG2). J Pharm Sci. 2006;95:1967–83.
7. Chari R, Jerath K, Badkar AV, Kalonia DS. Long- and short-range electrostatic interactions affect the rheology of highly concentrated antibody solutions. Pharm Res. 2010;26:2607–18.
8. Saluja A, Kalonia DS. Nature and consequences of protein-protein interactions in high protein concentration solutions. Int J Pharm. 2008;358:1–15.
9. Cromwell MEM, Felten C, Flores H, Liu J, Shire SJ. Self-association of therapeutic proteins: Implications for product development. In: Murphy RM, Tsai AM, editors. Misbehaving proteins: protein misfolding, aggregation, and stability, New York: Springer; 2006. pp 313–330.
10. Cleland JL, Powell MF, Shire SJ. The development of stable protein formulations: a close look at protein aggregation, deamidation and oxidation. Crit Rev Ther Drug Carr Syst. 1993;10:307–77.
11. Braun A, Kwee L, Labow MA, Alsenz J. Protein aggregates seem to play a key role among the parameters influencing the antigenicity of interferon alpha (INF-alpha) in normal and transgenic mice. Pharm Res. 1997;14:1472–8.
12. Hermeling S, Crommelin DJ, Schellekens H, Jiskoot W. Structure-immunogenicity relationships of therapeutic proteins. Pharm Res. 2004;21:897–903.
13. Robert D, Barelli S, Crettaz D, Bart PA, Schifferli JA, Betticher D *et al.* Clinical proteomics: study of a cryogel. Proteomics. 2006;6:3958–60.
14. Yagi H, Takahashi N, Yamaguchi Y, Kato K. Temperature-dependent isologous Fab-Fab interaction that mediates cryocrystallization of a monoclonal immunoglobulin G. Mol Immunol. 2004;41:1211–5.
15. Narayanan J, Liu XY. Protein interactions in undersaturated and supersaturated solutions: a study using light and X-ray scattering. Biophys J. 2003;84:523–32.
16. Salinas BA, Sathish HA, Bishop SM, Harn N, Carpenter JF, Randolph TW. Understanding and modulating opalescence and viscosity in a monoclonal antibody formulation. J Pharm Sci. 2010;99:82–93.
17. Yadav S, Liu J, Shire SJ, Kalonia DS. Specific interactions in high concentration antibody solutions resulting in high viscosity. J Pharm Sci. 2010;99:1151–68.
18. Saluja A, Badkar AV, Zeng DL, Nema S, Kalonia DS. Ultrasonic storage modulus as a novel parameter for analyzing protein-protein interactions in high protein concentration solutions: correlation with static and dynamic light scattering measurements. Biophys J. 2007;92:234–44.
19. Saluja A, Kalonia DS. Application of ultrasonic shear rheometer to characterize rheological properties of high concentration solutions at microliter volume. J Pharm Sci. 2005;94:1161–8.
20. Saluja A, Badkar AV, Zeng DL, Kalonia DS. Ultrasonic rheology of a monoclonal antibody (IgG_2) solution: implications for physical stability of proteins in high concentration formulations. J Pharm Sci. 2007;96:3181–95.
21. Patel AR, Kerwin BA, Kanapuram SR. Viscoelastic characterization of high concentration antibody formulations using quartz crystal microbalance with dissipation monitoring. J Pharm Sci. 2009;98:3108–16.
22. Kanai S, Liu J, Patapoff TW, Shire SJ. Reversible self-association of a concentrated monoclonal antibody solution mediated by Fab-Fab interaction that impacts solution viscosity. J Pharm Sci. 2008;97:4219–27.
23. Sukumar M, Doyle BL, Combs JL, Pekar AH. Opalescent appearance of an IgG1 antibody at high concentrations and its relationship to noncovalent association. Pharm Res. 2004;21:1087–93.
24. Annunziata O, Asherie N, Lomakin A, Pande J, Ogun O, Benedek GB. Effect of polyethylene glycol on the liquid-liquid phase transition in aqueous protein solutions. Proc Natl Acad Sci USA. 2002;99:14165–70.
25. Asakura S, Oosawa F. On interactions between two bodies immersed in a solution of macromolecules. J Chem Phys. 1954;22:1255–6.
26. Jion AI, Goh LT, Oh SKW. Crystallization of IgG1 by mapping its liquid-liquid phase separation curve. Biotech Bioeng. 2006;95:911–8.
27. Ahamed T, Esteban BNA, Ottens M, van Dedem GW, van der Wielen LA, Bisschops MAT *et al.* Phase behavior of an intact monoclonal antibody. Biophy J. 2007;93:610–9.
28. Dumets AC, Chockla AM, Kaler EW, Lenhoff AM. Protein phase behavior in aqueous solutions: crystallization, liquid-liquid phase separation, gels, and aggregates. Biophys J. 2008;94:570–83.
29. Haruyama H, Ito S, Miyadai K, Takahashi T, Kawaida R, Takayama T *et al.* Humanization of the mouse anti-Fas antibody HFE7A and crystal structure of the humanized HFE7A Fab fragment. Biol Pharm Bull. 2002;25:1537–45.
30. Thomson JA, Schurtenberger P, Thurston GM, Benedek GB. Binary liquid phase separation and critical phenomena in a protein/water solution. Proc Natl Acad Sci USA. 1987;84:7079–83.
31. Baek SG, Magda JJ. Monolithic rheometer plate fabricated using silicon micromachining technology and containing miniature pressure sensors for N_1 and N_2 measurements. J Rheology. 2003;47:1249–60.
32. Pipe C, Kim NJ, McKinley G. Microfluidic Rheometery on a Chip. 2007 4th AERC, Italy

33. Schuck P. Size distribution analysis of macromolecules by sedimentation velocity ultracentrifugation and Lamm equation modeling. Biophys J. 2000;78:1606–19.
34. Tanaka T, Ishimoto C. Phase separation of a protein-water mixture in cold cataract in the young rat lens. Science. 1977;197:1010–2.
35. Ishimoto C, Tanaka T. Critical behavior of a binary mixture of protein and salt water. Phys Rev Lett. 1977;39:474–7.
36. Kato K, Sautes-Fridman C, Yamada W, Kobayashi K, Uchiyama S, Kim H *et al.* Structural basis of the interaction between IgG and Fcγ receptors. J Mol Biol. 2000;295:213–24.
37. Oda M, Uchiyama S, Noda M, Nishi Y, Koga M, Mayanagi M *et al.* Effects of antibody affinity and antigen valence on molecular forms of immune complexes. Mol Immunol. 2009;47:352–64.
38. Liu J, Andya JD, Shire SJ. A critical review of analytical ultracentrifugation and field flow fractionation methods for measuring protein aggregation. AAPS J. 2006;8:E580–9.
39. Pekar A, Sukumar M. Quantitation of aggregates in therapeutic proteins using sedimentation velocity analytical ultracentrifugation: practical considerations that affect precision and accuracy. Anal Biochem. 2007;367:225–37.
40. George A, Wilson WW. Predicting protein crystallization from a dilute solution property. Acta Crystallogr A. 1994;D50:61–365.
41. George A, Chiang Y, Guo B, Arabshahi A, Cai Z, Wilson WW. Second virial coefficient as predictor in protein crystal growth. Methods Enzymol. 1997;276:100–10.
42. Clark JI, Clark JM. Lens cytoplasmic phase separation. Int Rev Cytol. 2000;192:171–87.
43. Cromwell MEM, Carpenter JF, Scherer T, Randolph TW. Opalescence in antibody formulations is a solution critical phenomenon. Abstracts of Papers. 2008 236th ACS National Meeting, Philadelphia, PA, United States.
44. Cromwell MEM. Implications of phase separation on pharmaceutical development. 2009 AAPS National Biotechnology Conference, Seattle, WA, United States.
45. McDonald P, Victa C, Carter-Franklin JN, Fahrner R. Selective antibody precipitation using polyelectlyte: A novel approach to the purification of monoclonal antibodies. Biotech Bioeng. 2009;102:1141–51.
46. Matheus S, Friess W, Schwartz D, Mahler HC. Liquid high concentration IgG1 antibody formulations by precipitation. J Pharm Sci. 2009;98:3043–57.
47. Strandner A, Sedgwick H, Cardinaux F, Poon WCK, Egelhaaf SU, Schurtenberger P. Equilibrium cluster formation in concentrated protein solutions and colloids. Nature. 2004;432:492–5.